Appl. Phys. 8, 151—162 (1975)

Applied Physics

Investigation of the Electronic Structure of Ferro- and Paramagnetic Nickel by Positron Annihilation

G. Kontrym-Sznajd and *H. Stachowiak*
Institute for Low Temperature and Structure Research, Polish Academy of Sciences
50-329 Wrocław, Plac Katedralny 1, Poland

*W. Wierzchowski**
Institute of Exp. Physics, University of Wrocław
50-205 Wrocław, Ul. Cybalskiego 36, Poland

K. Petersen, *N. Thrane*, and *G. Trumpy*
Laboratory of Applied Physics II, The Technical University of Denmark
DK-2800 Lyngby, Denmark

Received 2 May 1975/Accepted 5 June 1975

Abstract. Positron angular correlation curves have been measured for nickel in the [100], [110], and [111] directions at room temperature, 330° C and 380° C. Mijnarends' approach is used for their interpretation. For ferromagnetic nickel the 6th zone Fermi Surface (FS) obtained in this way is similar to that obtained from other experimental measurements as well as from band structure calculations. At 380° C the regrouping of the 5th zone electrons at the Curie point is well visible, and information is obtained about the paramagnetic nickel FS in the 6th and 5th zones. Besides, at this temperature the FS in the 6th zone is larger and rounded off. This effect, still needing further experimental confirmation, is attributed to thermal vibrations of the lattice.

Index Headings: Positron annihilation — Fermi surface — Ferromagnetic transition

The electronic structure of nickel has attracted considerable interest because of the magnetic properties of this metal.

There have been many band-structure calculations performed using different methods. The general features of the calculated Fermi Surfaces (FS) are qualitatively similar to each other [1–5]. The experimental results obtained mainly from the de Haas van Alphen effect, magnetoresistance and Azbel-Kaner cyclotron resonance confirmed the existence of a copper-like FS in the 6th majority spin band as well as of hole pockets at X in the 4th minority spin band both predicted by theory. However, there are no experimental informations about the existence of FS in 5th and 6th minority spin bands except in [6], where the first and so far unique information about the existence of the 6th minority spin band FS was obtained.

As concerns the electronic structures of paramagnetic nickel very little research has been devoted to this problem. Theoretical calculations suggest that its FS in the 6th band is similar to that of noble metals [7]. In the 5th band a large electron sheet and in the 4th and 3rd bands small hole pockets around X should be present. As concerns experimental data they lack completely for the FS in paramagnetic nickel. It is well known that most of the experimental methods of investigating the FS require low temperature technique, and they cannot be used to investigate Ni in this phase.

* Present address: Institute of Physics, The Technical University of Wrocław, Wyspiańskiego 27, PL-50-370 Wrocław, Wybrzeże, Poland.

In this situation measurements of the angular correlation of positron annihilation quanta (ACPAQ) seemed to be a promising method of investigating the electronic structure of para- as well as ferromagnetic nickel. Unfortunately measurements taking advantage of the polarization of the positrons emitted from β-sources did not lead to particularly conclusive results.

The purpose of this paper is to study the electronic structure of nickel by means of ACPAQ at different temperatures as well in ferro- and paramagnetic states. The measuring set-up and experimental results are described in Section 1 and a preliminary interpretation is attempted. In Section 2 test calculations are performed showing how a strongly anisotropic FS is described with three lattice harmonics only. It is shown that though a neck in the FS is badly described in this way, nevertheless such an approach permits not only to detect a neck but even to distinguish a conical neck from a cylindrical one. Afterwards, the results obtained by applying Mijnarends' method to our experimental data are presented. Section 3 contains the interpretation of the $\varrho(\boldsymbol{p})$ curves obtained in this way.

1. Experimental Results and Preliminary Interpretation

Measurements were performed with a conventional long-slit geometry angular correlation set-up for positron studies. The annihilation photons were registered in NaI(Tl) counters placed behind lead slits with openings 2 mm × 100 mm. Each slit was situated 2 m away on either side of the sample. Thus, the resolving power of the instrument was about 1 mrad. The samples were single crystal pieces of Ni having surface areas 1.5 cm × 1.0 cm facing the positron source which consisted of about 20 mCi of ^{58}Co. The sandwich source-sample geometry was used.

The registration of counts and coincidences, and the changing of angle between the detector arms were performed automatically, and in such a way that each coincidence curve could be scanned several times. The number of coincidence counts at the peak of the curve was about 15000 for each of the measurements performed in this work.

Angular correlation curves have been obtained for nickel samples oriented in the directions (100), (110), and (111) oriented normally to the slit system of the instrument. Measurements were performed at room temperature, at 330° C and at 380° C. The latter temperatures lie below and above the Curie point at

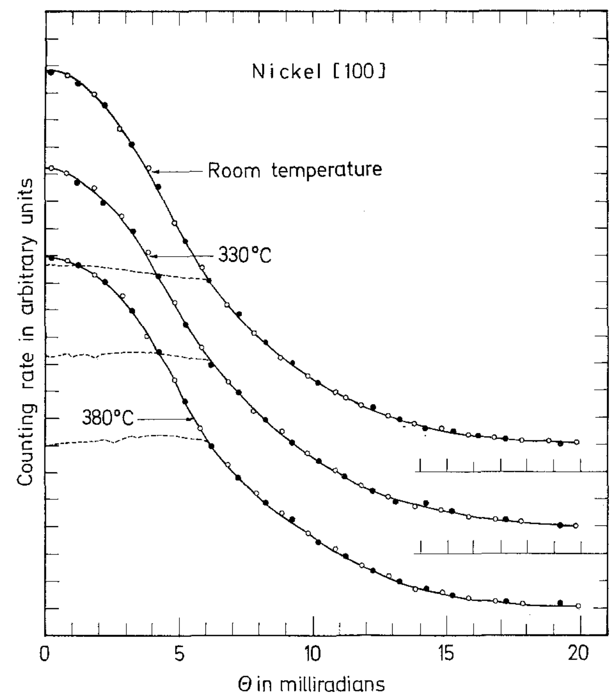

Fig. 1. Experimental angular correlation curves for the (100) direction. The black and white circles correspond to positive and negative angles. The core contribution is indicated by the dotted line

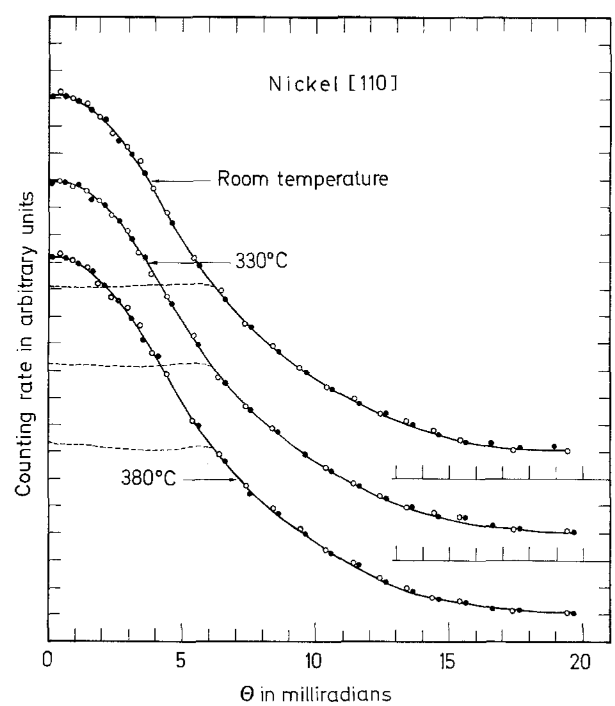

Fig. 2. The same as in Fig. 1, but for the [110] direction

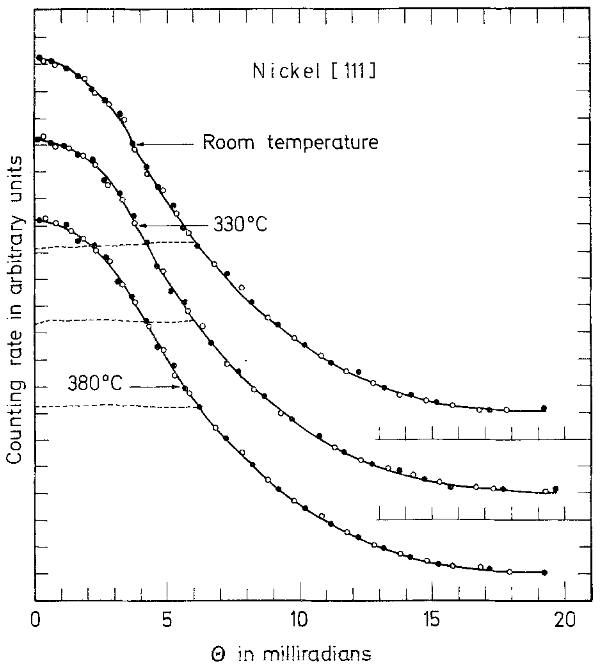

Fig. 3. The same as in Fig. 1, but for the [111] direction

$T_c = 361°$ C. All measurements were performed in argon atmosphere. The temperature was stable within $\pm 1°$ C.

The experimental curves are shown in Figs. 1–3. The scattering in the experimental points is due to the finite number of coincidences registered.

Comparison of the annihilation curves obtained for a given direction at various temperatures shows significant changes, different in character from those observed by many investigators who studied the influence of temperature on the angular distribution of annihilation quanta [8–11]. In our case the most important conclusion is that the annihilation curves do not change monotonically, when the temperature increases. So one can conclude that the Curie transition alters the electronic structure of nickel and this fact is mainly responsible for the observed changes of the annihilation curves. On the other hand, the annihilation curves measured at a given temperature for three crystallographical directions show a marked anisotropy caused by the anisotropy of the FS of nickel. We have plotted in Figs. 4 and 5 the experimentally obtained difference curves $N_{[100]}(\theta) - N_{[111]}(\theta)$ and $N_{[110]}(\theta) - N_{[111]}(\theta)$ (for room temperature) together with the relevant parts of the ferromagnetic nickel FS proposed by Callaway and Zhang [2] projected onto the plane of the drawing. We chose the results of this

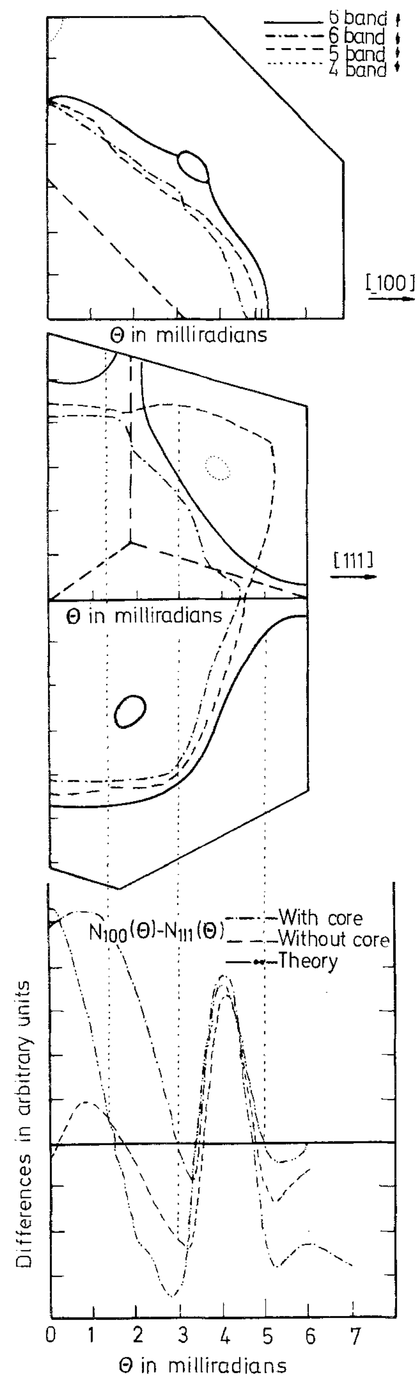

Fig. 4. ACPAQ difference curves: $N_{[100]}(\theta) - N_{[111]}(\theta)$ as follow from the 6th zone FS cross-sections (—·—) and from experiment before (—·—) and after (– – –) subtracting the contribution from HMC and core annihilation

paper because they interpolate pretty well the numerous FS's obtained by different authors. In these figures the same difference curves are also shown after subtracting the core contribution. The core contribution has been

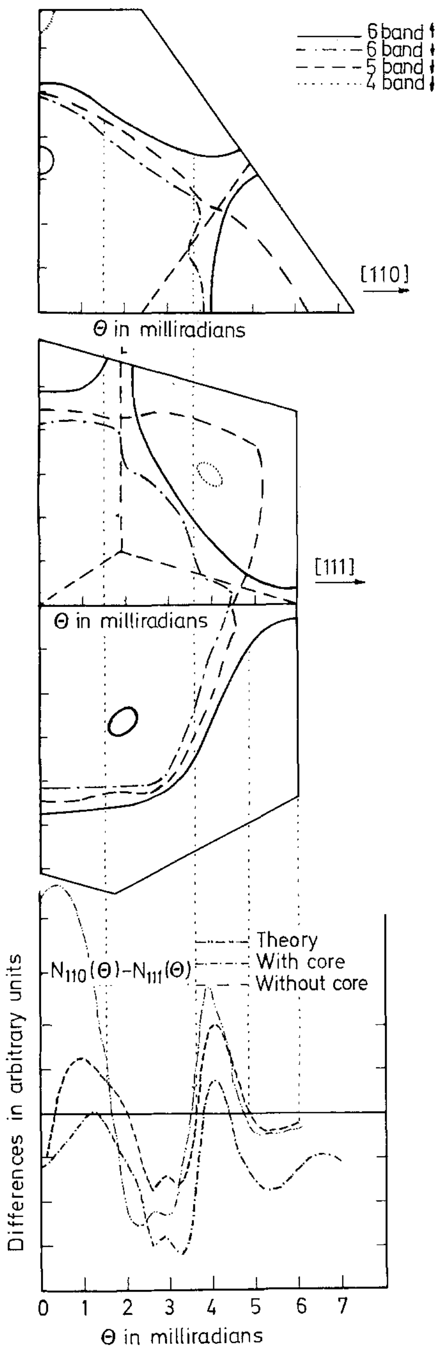

Fig. 5. The same as in Fig. 4, but for $N_{[110]}(\theta)-N_{[111]}(\theta)$

calculated in the way proposed by Stachowiak [12]. On the basis of the FS proposed in [2] we have computed the FS cross-sectional curves by assuming a constant electron density inside the FS. From Figs. 4 and 5 general agreement is visible between the difference curves without core contribution and the calculated ones. Careful inspection of the former shows that their overall behaviour stems principally from the shape of the ferromagnetic nickel FS. This fact is in contradiction to the work of Shiotani *et al.* [13]. Especially the minima in the range of 5–6 mrad clearly reflect the existence of a neck. The deviations at small angles can be due to the contributions from the 5th zone electrons and 4th zone holes. In calculating the "theoretical" curves we have taken into account only the 6th zones neglecting electrons in lower zones. In spite of that it seems that the agreement of the experimental curves with the calculated ones is perhaps better than in the case of copper in which the FS exists only in the first zone [14].

Unfortunately because of the lack of suitable information about the FS we are unable to compare the experimental results obtained at 330° C and 380° C to the shapes of the FS of nickel at these temperatures. Subsequently we have used Mijnarends' approach [15] to the interpretation of our results.

2. Calculation of the Electron Density $\varrho(p)$

Nickel crystallizes in the *fcc* structure. The lattice harmonics for this structure can be found in [16–18]. In order to describe the momentum density distribution $\varrho(\boldsymbol{p})$ we take the first three lattice harmonics according to [18]. Neglecting the factor $(4\pi)^{-\frac{1}{2}}$ we have

$$F_0(\theta,\phi)=1\,,$$

$$F_4(\theta,\phi)=0.76376261C_4^0(\theta,\phi)+0.64549722C_4^4(\theta,\phi)\,,$$

$$F_6(\theta,\phi)=0.35355338C_6^0(\theta,\phi)-0.93541434C_6^4(\theta,\phi)\,,$$

where

$$C_l^{|m|}(\theta,\phi)=\begin{cases}[(2l+1)(l-|m|)!/2\pi(l+|m|)!]^{\frac{1}{2}}\mathrm{P}_l^{|m|}(\cos\theta)\cos m\phi & \text{for } m\neq 0\\ [(2l+1)/4]^{\frac{1}{2}}\mathrm{P}_l(\cos\theta) & \text{for } m=0\end{cases}$$

and $\mathrm{P}_l^{|m|}(\cos\theta)$ are associated Legendre polynomials. Figures 6–8 show $\varrho(\boldsymbol{p})$ along the crystallographical directions that have been investigated experimentally

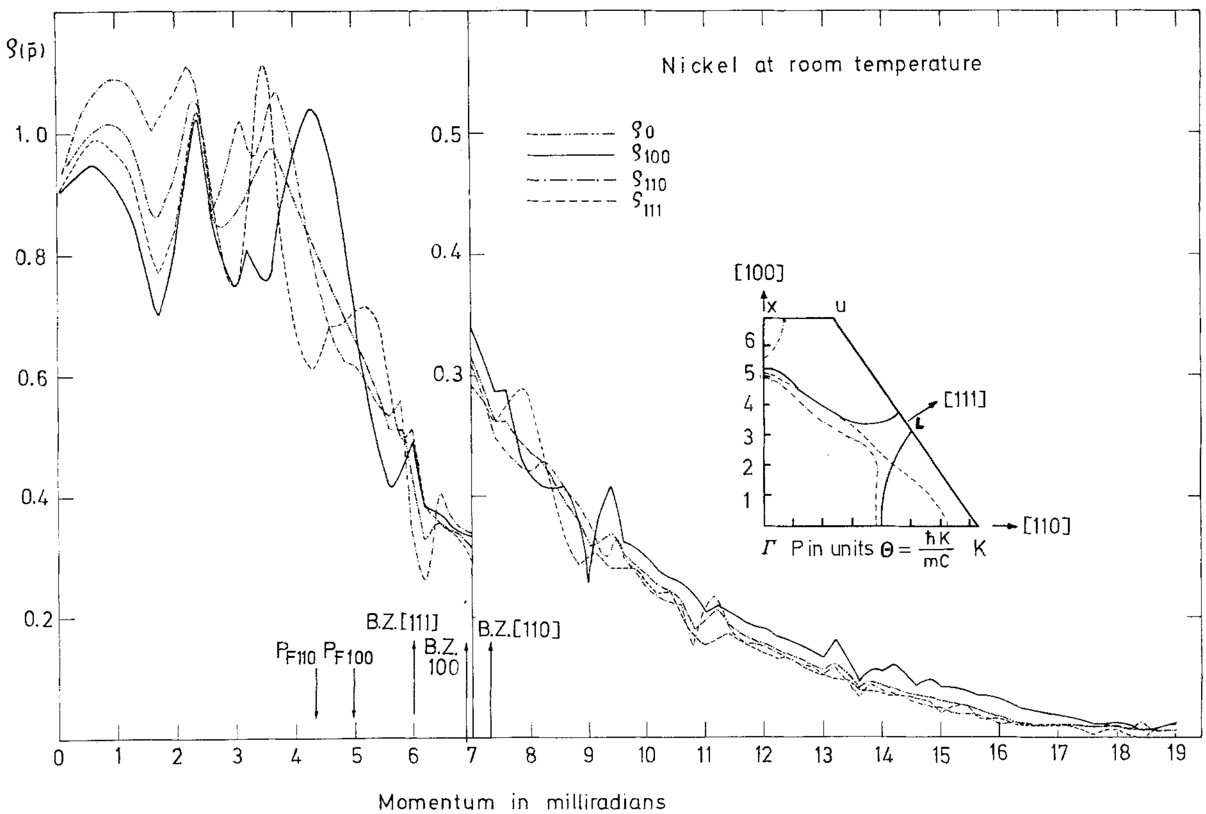

Fig. 6. The electronic density along the main crystallographical directions as obtained for ferromagnetic nickel (room temperature) using Mijnarends' approach. The insertion shows the FS in the [110] plane

for room temperature, 330° C and 380° C, respectively.

First, test calculations have been performed concerning how far, for metals having a strongly anisotropic FS, the function $\varrho(\boldsymbol{p})$ is determined with three lattice harmonics only. For this purpose we assumed the following three models of FS

1) Spherical central part (belly) with cylindrical necks in the [111] direction.
2) The same central part shape with truncated cone necks in the [111] direction.
3) Central part the same as in 1) and 2) with bumps in the [100] direction.

Then we computed the cross-sectional curves $N(p_z)$ for the [100], [110], and [111] directions and for each of these models independently. In our calculations we took into account only the necks and bumps as elements causing the anisotropy of the FS. The cross-sections $N(p_z)$ obtained in this way served for calculating "theoretical" $\varrho(\boldsymbol{p})$ curves in the main crystallographical direction (Fig. 9). Their analysis shows that the necks indeed manifest in the [111] direction and the bumps in the [100] direction. There are also, however, maxima and minima in the "theoretical" $\varrho(\boldsymbol{p})$ curves showing that the description of the neck with three lattice harmonics gives rise to additional features. Since, however, the approximate shape of the FS is known the confrontation of the "theoretical" $\varrho(\boldsymbol{p})$ curves with those obtained from experiment at room temperature can answer the question, whether the minima and maxima existing in the experimental $\varrho(\boldsymbol{p})$ functions are caused by bumps or necks of the FS. Finally we can conclude that the neck in the [111] direction and the bump in the [100] direction exist in ferromagnetic nickel. Moreover, as can be seen from Figs. 6 and 9 there is a much better agreement of the experimental curves $\varrho(\boldsymbol{p})$ to the theoretical ones calculated for conical necks than to those resulting from cylindrical ones. So, such test calculations can be useful for detecting a neck and determining its shape as well as other details of the FS.

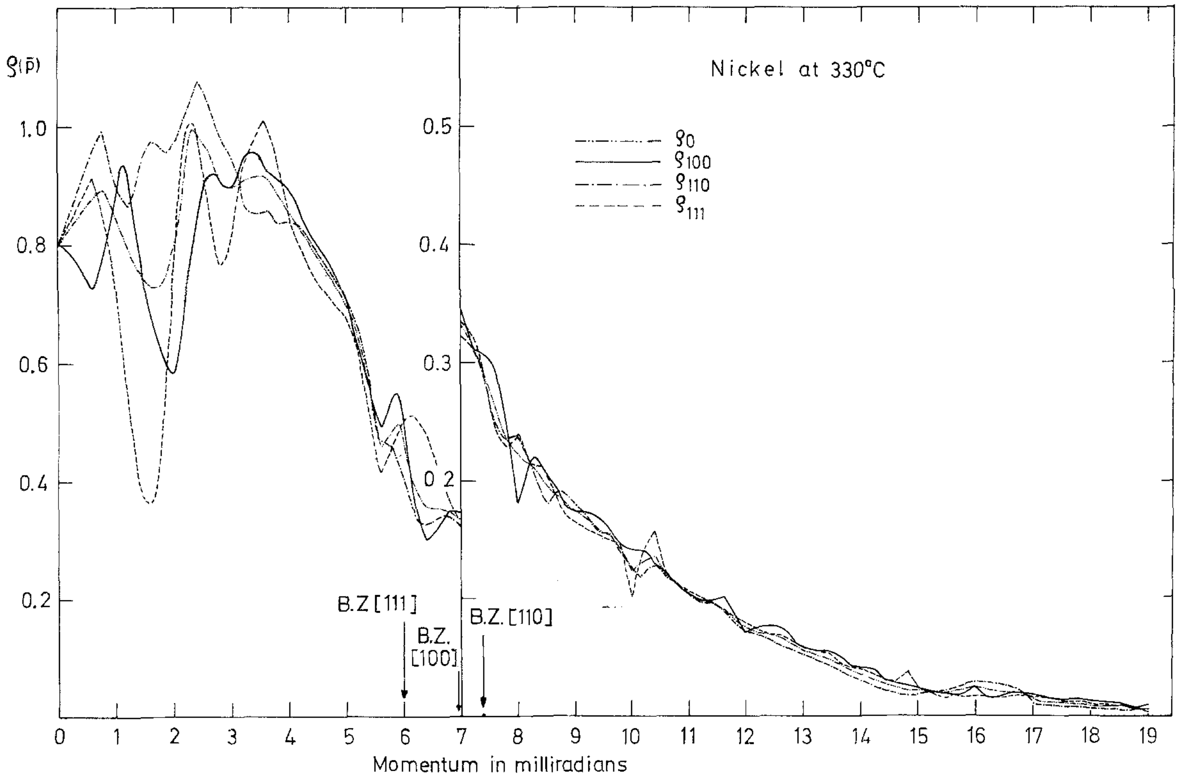

Fig. 7. The same as in Fig. 6, but for 330° C

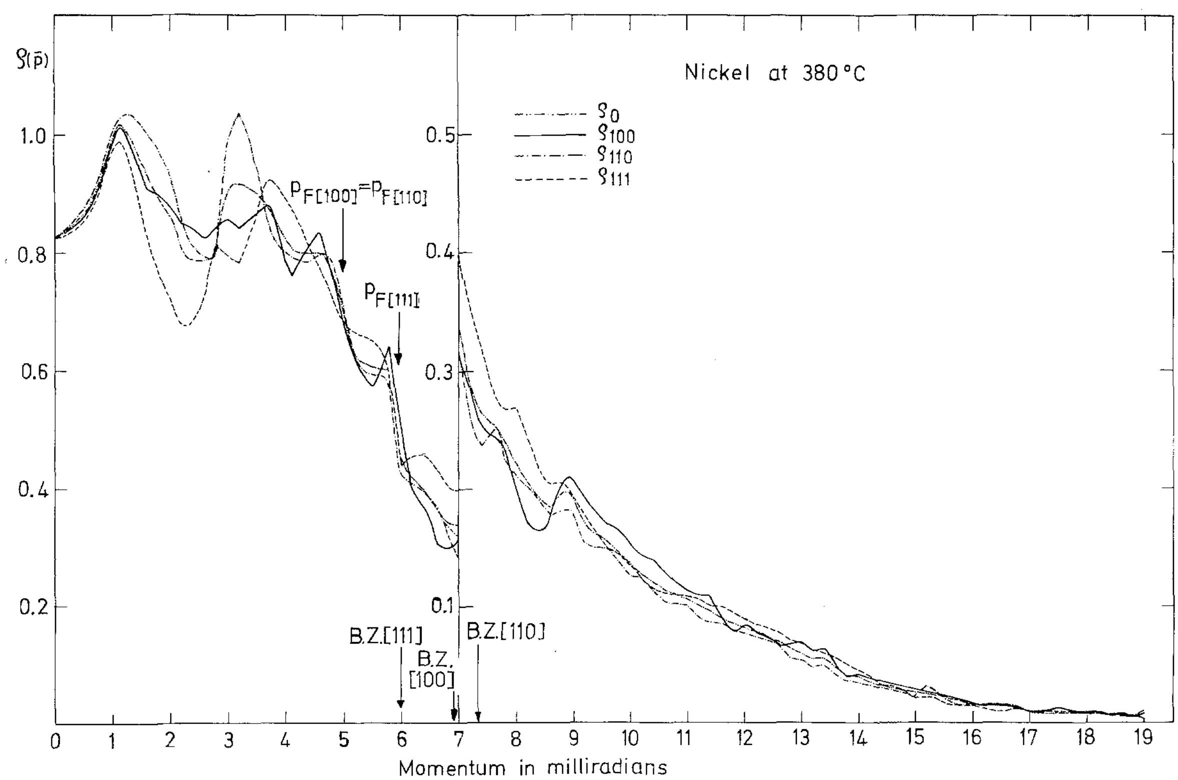

Fig. 8. The same as in Fig. 6, but for 380° C (paramagnetic state)

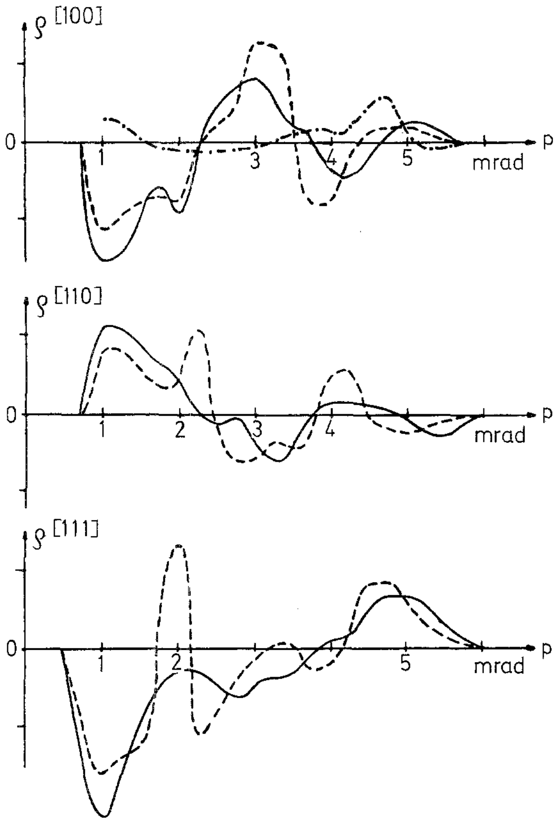

Fig. 9. The "test" electron density calculated from three FS models: (——) model 1, (– – –) model 2, (–·–·–) model 3

3. Interpretation

3.1 Nickel at Room Temperature

The density of states $\varrho(\boldsymbol{p})$ along three crystallographical directions obtained from our experiment is shown in Fig. 6. The high peaks at $\theta = 4.3$ mrad and $\theta = 3.7$ mrad for the [100] and [110] directions, respectively, are assumed to reflect the effect of enhancement. It is not well known, how far Kahana's theory [19] holds in real metals, but from our $\varrho(\boldsymbol{p})$ curves it seems that the enhancement factor is isotropic in the [100] and [110] directions. The maximum at $\theta = 5.0$ mrad in the [111] direction is assumed to reflect the existence of the neck. The peak of this curve at $\theta = 5.7$ mrad can also be considered as a Fujiwara type enhancement [20–22] appearing when the FS touches the Brillouin zone boundary.

The experimental density of states $\varrho(\boldsymbol{p})$ should contain informations about features like FS bumps, depression and necks. The results are more visible if one draws isodenses (curves of equal density). The bump in the [100] direction and a depression in the [110] direction for the 6th band the FS are well seen (Fig. 10). As important bulging ascribed by us to the neck is visible in the [111] direction.

Since due to the enhancement the real $\varrho(\boldsymbol{p})$ function is not constant on the Fermi surface, we do not use the isodense to reconstruct the FS.

Now we use the experimental density curves $\varrho(\boldsymbol{p})$ to determine the 6th majority spin band fermi radii (in Fig. 6 these functions are shown along the main crystallographical directions only). This we do by finding the bottom and the top of the slope of $\varrho(\boldsymbol{p})$ at p_F and measuring the position of the centre of the slope. The FS in the 6th majority spin band obtained finally from our experimental data is presented in Fig. 12. All characteristic details, such as FS bumps, depressions and necks predicted by theory and suggested in experiment [1] are clearly seen. The radius of the neck at the Brillouin zone boundary has been taken equal to about 0.3 mrad according to the de Haas van Alphen data for ferromagnetic nickel [23–25]. However, it should be pointed out here that one cannot describe properly a neck with three lattice harmonics only. So our results concerning the neck must be treated with caution.

It is tempting to consider the sharp maximum at $\theta \approx 3.5$ mrad in the density curve along the [111] direction as responsible for the minority spin FS in 6th band (we do not observe such a maximum in the test curve—Fig. 9). In this direction both the minority and majority spin FS in 6th bands are far enough from each other to be distinguished in our experiment. The FS of 6th minority spin band obtained in the same way as previously described for majority spin is also presented in Fig. 11. For other directions both sheets of the FS in 6th band are close to each other what makes it impossible to determine the Fermi radii, though we suspect that the small maxima at $\theta \approx 3.2$ mrad and at $\theta \approx 3.0$ mrad for the [100] and [110] directions, respectively, may follow from the minority spin FS in 6th band also in directions different from [111]. For the same reason we are unable to determine the FS in 5th band except in the ΓK direction, where we get the FS at 6.1 mrad by assuming that the sharp drop of the density of states at $\theta \approx 6$ mrad reflects the presence of a minority FS.

3.2 Nickel at Higher Temperatures

The annihilation curves obtained at 330° C, i.e. below the Curie point, have been interpreted in the same way as above. The density of states $\varrho(\boldsymbol{p})$ obtained from

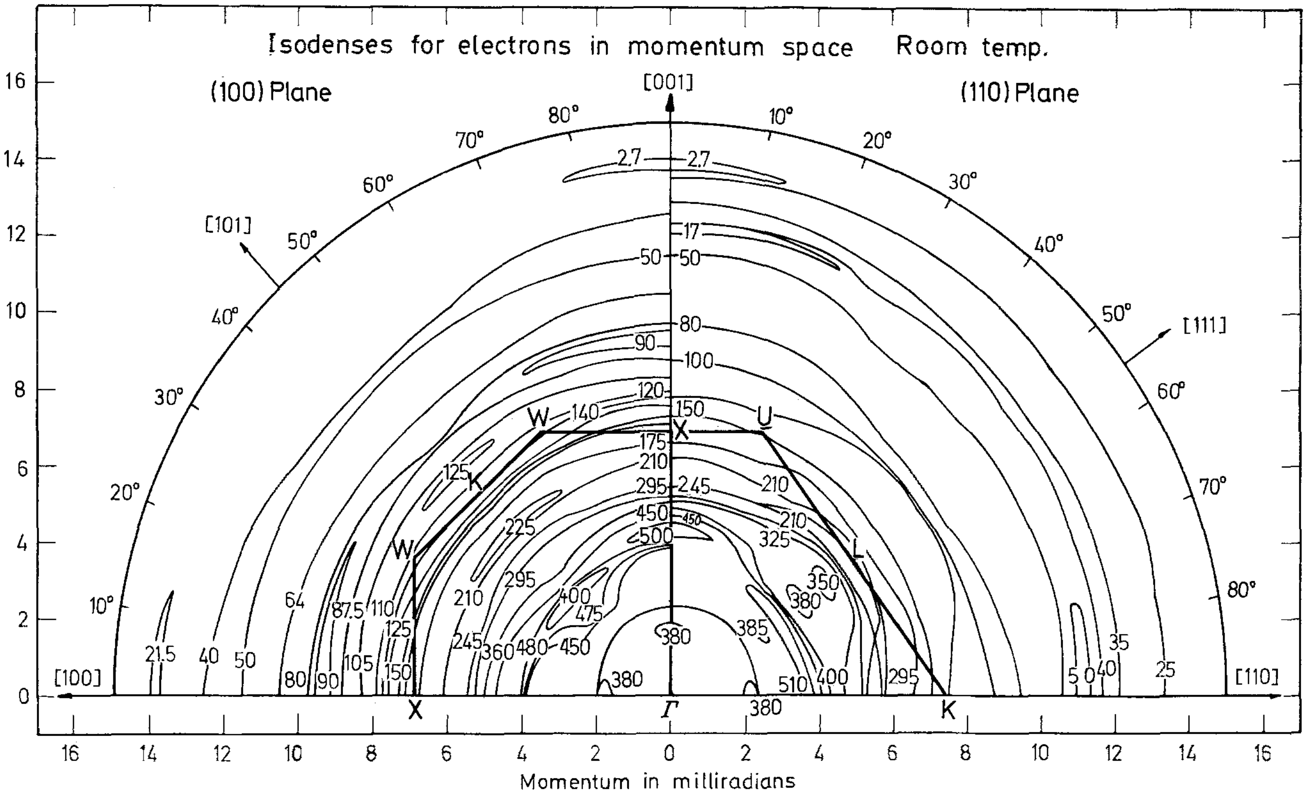

Fig. 10. Isodenses for ferromagnetic nickel (room temperature)

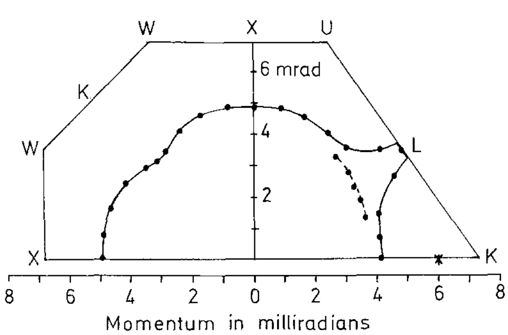

Fig. 11. The 6th zone FS for ferromagnetic nickel as follows from this work. In the [111] direction the FS is shown for both majority and minority spin. The points on the surface have been obtained from our experimental data. The asterisk indicates the Fermi radius in the 5th zone towards K

experimental data is shown in Fig. 7 for 330° C and in Fig. 8 for 380° C. It is visible at first sight that the features of the density of states at the FS smear out at 330° C and they become sharp again above the Curie temperature. This suggests that the electronic structure of nickel does not change monotonically during the Curie transition. The isodenses for 380° C are shown in Fig. 12. For paramagnetic nickel the main contribution to positron annihilation should come from the 6th and 5th bands where there are sheets of the FS. The lower bands are filled except perhaps for small hole pockets around X in the 4th zone. This FS should have an analogy to that of palladium [26] except that in Pd there are 1.64 electrons per atom in the 5th band against 0.36 in the 6th band, while in Ni there are approximately 1.4 electrons in the 5th band and 0.6 in the 6th band. So in comparison with palladium the 5th FS of nickel should be smaller and the 6th band FS should be bigger. With regard to the ferromagnetic phase the occupied majority spin states in the 5th zone should empty for momentum close to the Brillouin zone boundary. Figure 13 in which the difference isodenses between 380° C and room temperature are shown confirms the above expectations. In the shaded areas $\varrho_{380°C}(p) > \varrho_{RT}(p)$ (RT: room temperature). The transfer of the 5th zone electrons from the areas (unshaded) close to the Brillouin zone boundary to those with lower momenta (shaded areas) as well as the separation of the 6th zone FS from that in the 5th zone are well seen. For reconstructing the 6th zone FS the derivatives of the

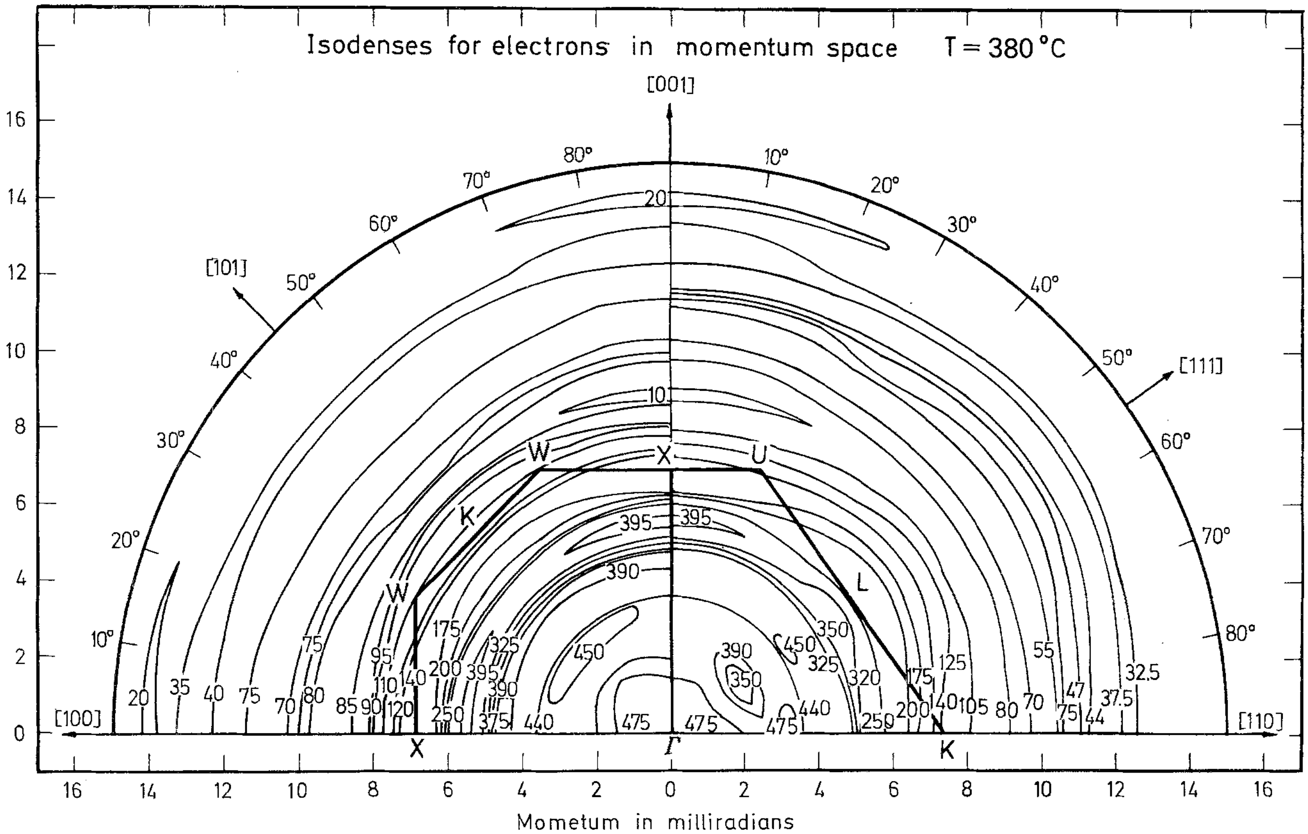

Fig. 12. Isodenses for paramagnetic nickel (380° C)

experimental annihilation curves were very helpful. For the values of θ at which the sign of $d^2N(\theta)/d\theta^2$ changes, there is a small maximum in the density curves $\varrho(\boldsymbol{p})$ at $\theta \approx 4.5$ mrad in the [100] direction, and "plateaus" from $\theta \approx 4.0$ mrad to $\theta \approx 5.75$ mrad in the [111] direction. These features were assumed to reflect the shape of the FS. The 6th band FS obtained in this way (Fig. 14) seems to be isotropic between the axes Δ and Σ. We cannot decide whether there is a neck at L or not. Also the difference isodenses cannot give any proof of the existence of a neck. As we know the shaded areas were explained as a result of regrouping of the 5th band electrons. There are shaded areas around L in the difference isodenses, but this fact does not exclude the existence of a neck in the paramagnetic state, because the neck range in this state is occupied by electrons with both spins against one spin only in the ferromagnetic state. Probably the neck exist at L, but its shape must be different from that in the ferromagnetic phase. Such a conclusion follows from the comparison of the test $\varrho(\boldsymbol{p})$ curves to those obtained from experimental data at 380° C. If a neck exists then the 6th zone FS of paramagnetic nickel is similar to that of copper.

It should be noted here that the volume of our paramagnetic FS is bigger than expected. Our results interpreted in the usual way would give about 0.96 electrons per atom in the 6th zone against 0.6 in the ferromagnetic state and about 1.68 in the 5th zone instead of 1.4. From the difference isodenses $\varrho_{380^\circ\mathrm{C}}(\boldsymbol{p}) - \varrho_{\mathrm{RT}}(\boldsymbol{p})$ one can see that the apparent electron density in paramagnetic Ni decreases for momenta inside the 6th zone FS. Also the 6th zone FS is more spherical in the paramagnetic than in the ferromagnetic state. Since the total number of electrons should be constant, our results suggest that the bulk of the FS is porous. The FS is measured usually at low temperature and it is believed that it remains essentially unchanged when the temperature rises, because of the high degeneracy of the electron gas. Such an approach, however, does not take into account distortions of the lattice connected with thermal vibrations. These can probably lead to local fluctuations of the FS. We are inclined at present to attribute our results to this

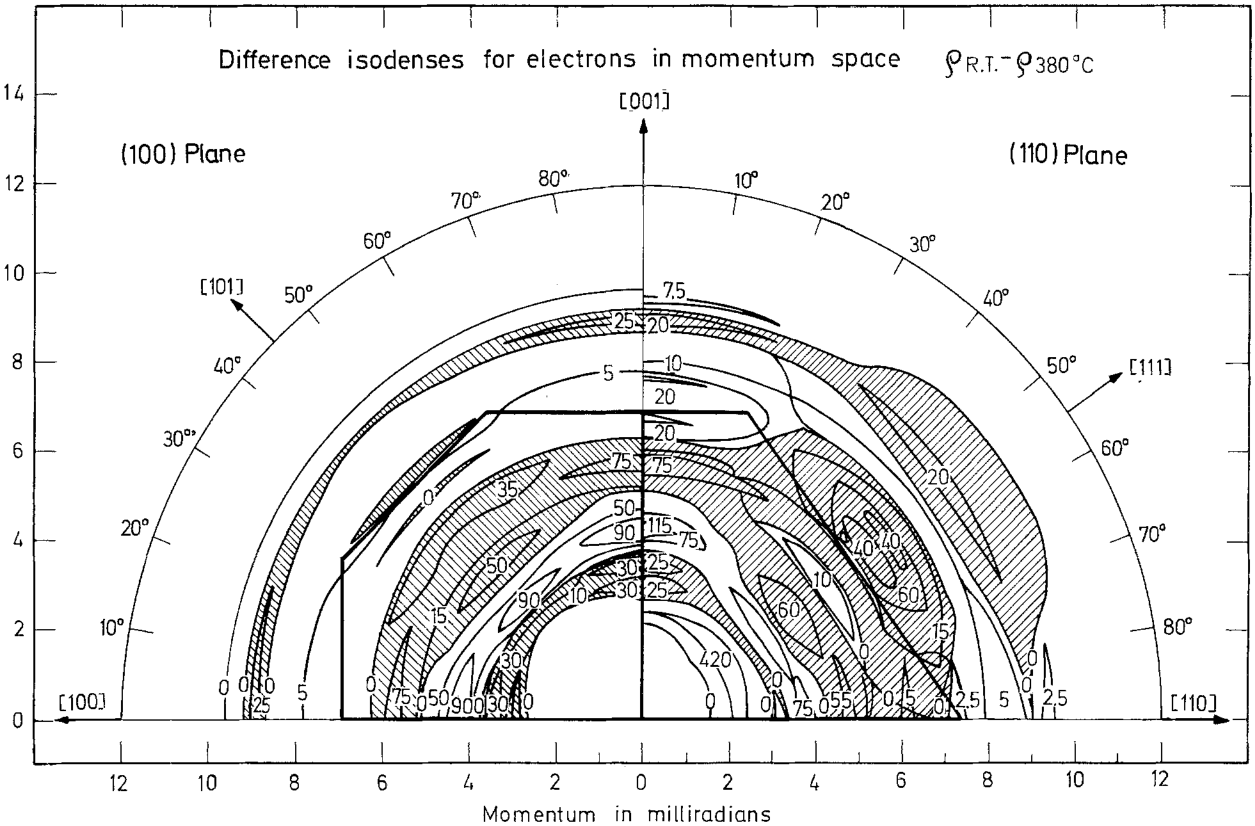

Fig. 13. Difference isodenses between 380° C and room temperature. The shaded areas show where the electron density has increased as a result of transition from the ferromagnetic to the paramagnetic state

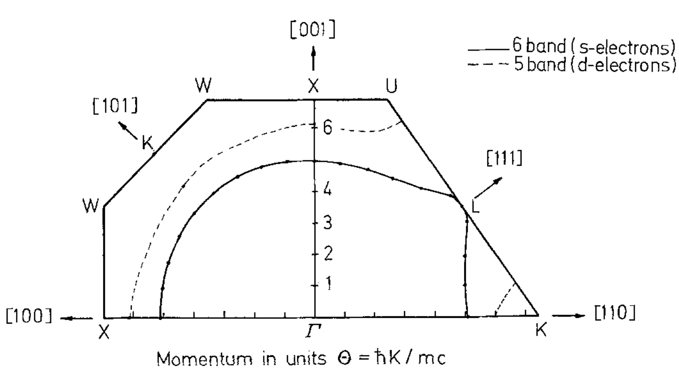

Fig. 14. The FS for paramagnetic nickel as obtained in this work

effect. Of course, this point needs further experimental and also theoretical investigation.

It should be noted that the dimensions of the FS in copper obtained by Mijnarends [27] are also higher in comparison to those obtained from the de Haas-van Alphen effect (see Ref. [27], Fig. 6), i.e. at liquid helium temperature as well as from elementary considerations.

As concerns the 5th band FS we are able to estimate the Fermi radii in the [100] and [110] directions only by assuming that the sharp dose of $\varrho(\boldsymbol{p})$ at $\theta \approx 5.8$ mrad for the [100] direction and at $\theta \approx 6.0$ mrad for the [110] direction indicate the position of the FS. Then using the difference isodense picture we propose the approximated shape of the 5th band FS (see Fig. 14). For nickel in comparison with palladium let us point out that the points K and U are empty in the 5th zone and the FS is open.

Unfortunately we are unable to reach any reasonable conclusion from our experimental data for 330° C, except for the smearing of the electron density in the neighbourhood of the FS, due to spin disorder. There exist visible a bump toward X, a depression in the [110] direction and a neck at L (Fig. 15), but the values of momenta corresponding to them are higher than for nickel at room temperature. The difference isodenses comparing the density of states at 330° C and room temperature (Fig. 16) did not help us to understand the situation below the Curie point.

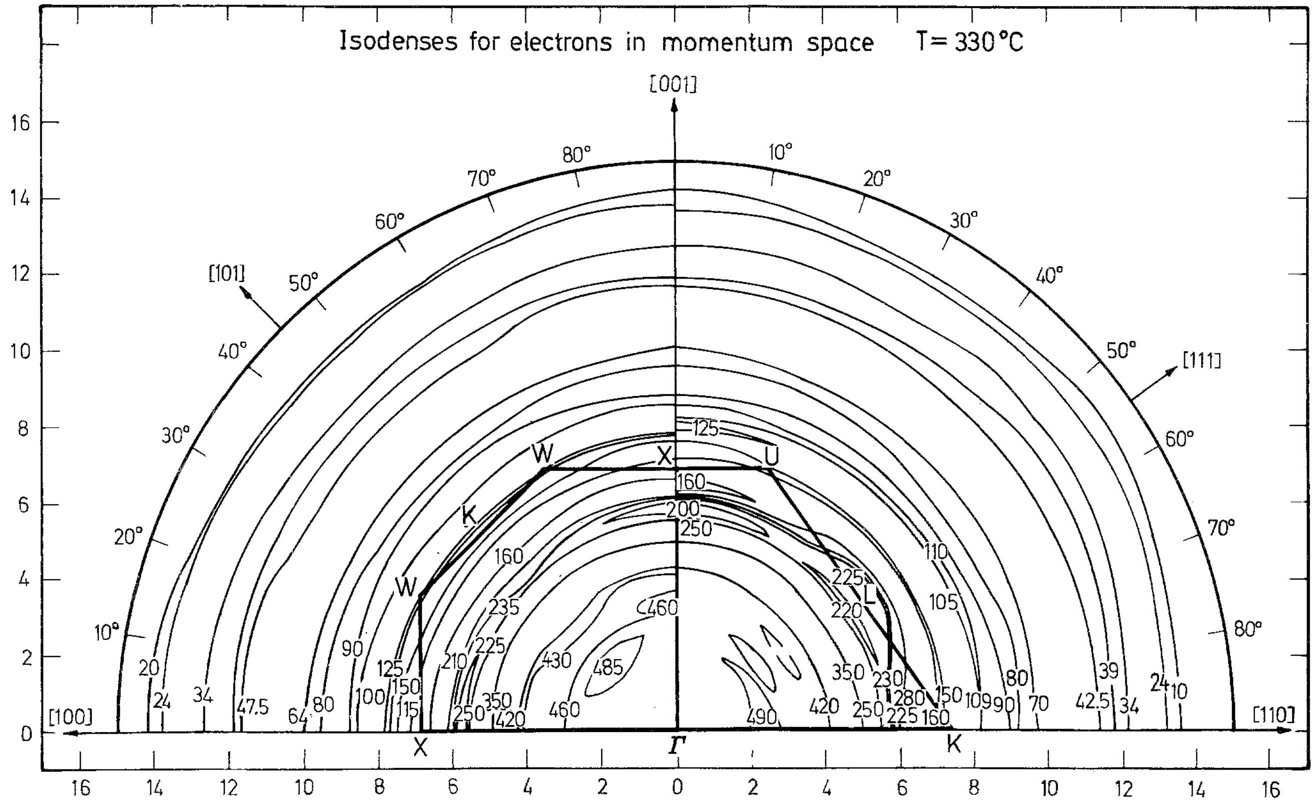

Fig. 15. Isodenses for nickel at 330 C

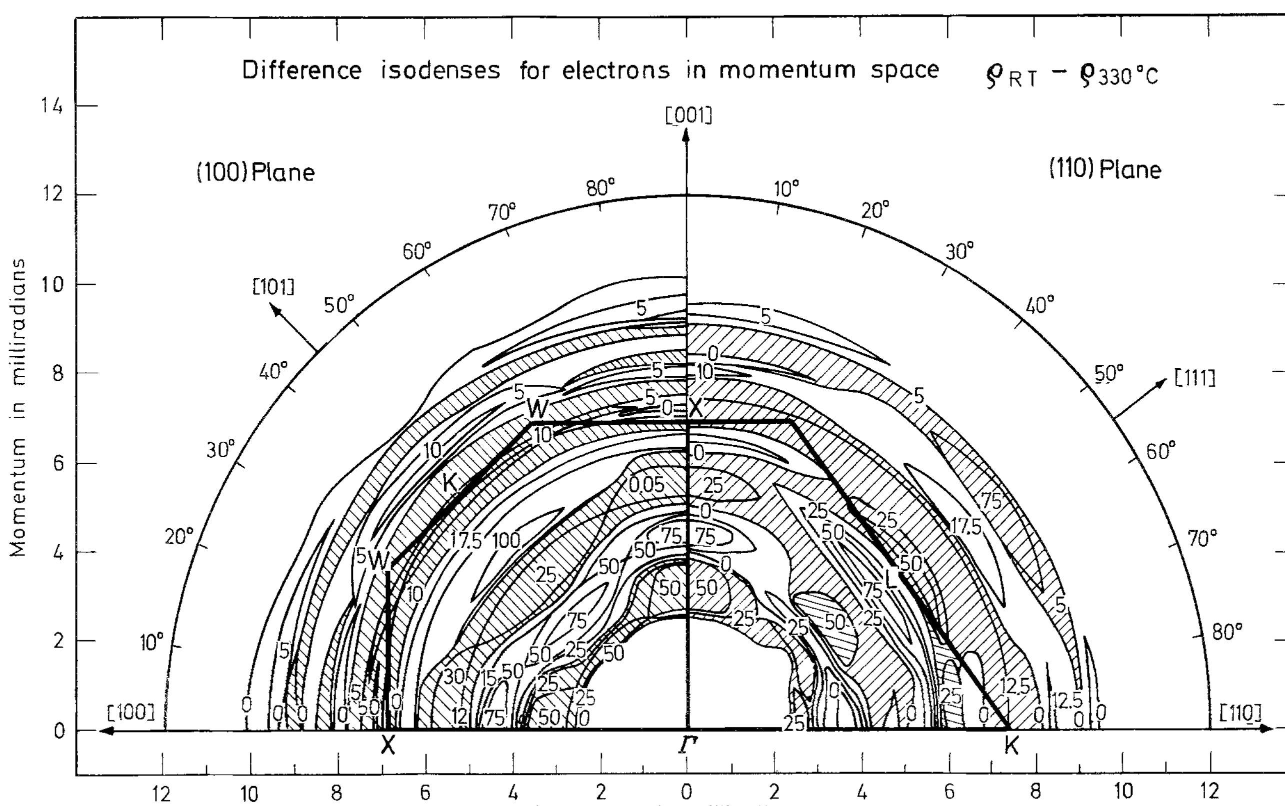

Fig. 16. Difference isodenses comparing the electron density at 330° C and room temperature

Nevertheless we feel that a detailed investigation of annihilation curves in the vicinity of the Curie point would constitute a powerful tool in studies of the ferromagnetic transition.

Conclusions

Mijnarends' way of interpreting our experimental results allowed to obtain the 6th zone majority spin FS of ferromagnetic nickel which is in qualitative agreement with the one computed theoretically. The comparison of our experimental results with the curves obtained theoretically by Singru and Mijnarends [28] shows that the enhancement following from positron interaction with the electron gas plays an important role in detecting the Fermi surface which in the independent particle approximation would hardly be visible.

The first experimental informations concerning the existence of the bulging toward X and the depression in the ΓK direction have been obtained. Moreover, our experimental data for room temperature show that the neck in the FS has rather a conical than a cylindrical shape.

There is a good agreement between the theoretical FS cross-section difference curves and those obtained experimentally.

Some suggestions concerning properties of the 6th and 5th minority FS have been obtained.

As concerns the paramagnetic state we have reconstructed the Fermi surfaces in the 6th and 5th zones. Both are bigger and rounded off in comparison to the ferromagnetic state. This is a new effect which we suppose to be a result of thermal lattice vibrations. However, this problem needs confirmation in further experiments. We also observe the regrouping of electrons in the 5th zone in comparison to room temperature due to the Curie transition.

As concerns our results for 330° C they suggest non-monotonic changes of the electronic structure during transition from ferro- to paramagnetic state. In this context the data below the Curie point are of particular interest from the point of view of the nature of the ferromagnetic transition, but their interpretation is rather difficult at this stage.

We feel that research with use of the positron annihilation method should continue in the following directions: 1) Measurements should be performed for more crystallographical directions. 2) The ferro-paramagnetic phase transition should be studied by ACPAQ in the immediate neighbourhood of the Curie temperature. 3) The temperature changes of the Fermi Surface require more detailed investigations on metals, which do not undergo phase transitions in the investigated temperature interval.

Acknowledgement. One of us (W.W.) is very grateful to the Danish Research Fund for Natural Sciences for support during his stay at the Technical University of Denmark.

References

1. A.P.Cracknell: *The Fermi Surface of Metals* (Taylor and Francis LTD., London 1971)
2. J.Callaway, H.M.Zhang: Phys. Rev. B, **1**, 305 (1970)
3. J.Langlinais, J.Callaway: Phys. Rev. B, **5**, 124 (1972)
4. J.Callaway, C.S.Wang: Phys. Rev. B, **7**, 1096 (1973)
5. C.S.Wang, J.Callaway: Phys. Rev. B, **9**, 4897 (1974)
6. P.Goy, C.C.Grimes: Phys. Rev. B, **7**, 299 (1973)
7. J.Friedel: In *The Physics of Metals. I Electrons*, ed. by J.M. Ziman (Cambridge University Press, 1964) Chap. 8
8. I.K.MacKenzie, G.F.O.Longstroth, B.T.A.McKee, C.G. White: Can. J. Phys. **42**, 1837 (1964)
9. A.T.Stewart, J.B.Shand: Phys. Rev. Letters **16**, 261 (1966)
10. S.M.Kim, A.T.Stewart, J.P.Carbotte: Phys. Rev. Letters **18**, 385 (1967)
11. O.Mogensen, K.Petersen: Phys. Letters **30**A, 542 (1969)
12. H.Stachowiak: Phys. Stat. Sol. **41**, 599 (1970)
13. N.Shiotani, T.Okada, H.Sekizawa, T.Mizoguchi, T.Karasawa: J. Phys. Soc. Japan **35**, 456 (1973)
14. S.Berko, S.Cushner, J.C.Erskine: Phys. Letters **27**A, 668 (1968)
15. P.E.Mijnarends: Phys. Rev. **160**, 512 (1967)
16. F.C.Van der Lage, H.A.Bethe: Phys. Rev. **71**, 612 (1947)
17. S.L.Altman, A.P.Cracknell: Rev. Mod. Phys. **37**, 19 (1965)
18. F.M.Mueller, H.G.Priestly: Phys. Rev. **148**, 638 (1966)
19. S.Kahana: Phys. Rev. **129**, 1622 (1963)
20. K.Fujiwara: J. Phys. Soc. Japan **29**, 1479 (1970)
21. K.Fujiwara, T.Hyodo, J.Ohyma: J. Phys. Soc. Japan **33**, 1047 (1972)
22. G.Kontrym-Sznajd, H.Stachowiak: Appl. Phys. **5**, 361 (1975)
23. D.C.Tsui, R.W.Stark: Phys. Rev. **164**, 669 (1967)
24. A.S.Joseph, A.S.Thorsen: Phys. Rev. Letters **11**, 554 (1963)
25. D.C.Tsui, R.W.Stark: Phys. Rev. Letters **17**, 871 (1966)
26. F.M.Mueller, A.J.Freeman, J.O.Dimmock, A.M.Furdyna: Phys. Rev. B, **1**, 4617 (1970)
27. P.E.Mijnarends: Phys. Rev. **178**, 622 (1969)
28. R.M.Singru, P.E.Mijnarends: Phys. Rev. B, **9**, 2372 (1974)